Available online at www.sciencedirect.com

SciVerse ScienceDirect

Ceramics International 38 (2012) 3693–3699

CERAMICS INTERNATIONAL

www.elsevier.com/locate/ceramint

Two-step sintering assisted consolidation of bulk titania nano-ceramics by spark plasma sintering

Bao-rang Li *, Dong-yu Liu, Jing-jing Liu, Shi-xiang Hou, Zhi-wei Yang

Key Laboratory of Condition Monitoring and Control for Power, Plant Equipment of Ministry of Education, North China Electric Power University, Beijing 102206, China

Received 24 July 2011; received in revised form 19 December 2011; accepted 4 January 2012
Available online 21 January 2012

Abstract

This work investigates the feasibility to the fabrication of high density of nano-grained titanium dioxide ceramics by two-step sintering process under spark plasma conditions. First step is carried out by fast-heating-rate sintering in order to obtain an initial high density and a second step is held at a lower temperature by isothermal sintering aiming to increase the density without obvious grain growth. Experiments are conducted to determine the appropriate temperatures for each step. The temperature range between 840 and 850 °C is effective for the first step sintering (T_1) due to its highest densification rate. The isothermal sintering is then carried out at 810–830 °C (T_2) for various hours in order to avoid the abnormal grain growth and improve the density at the same time. TiO_2 bulk ceramics with nano-sized grain were fabricated successfully by combination of spark plasma sintering (SPS) with the two step sintering method (TSS). Titanium dioxide nano-ceramics with >95% theoretical density could be obtained with T_1 and T_2 taken as 850 °C and 830 °C, respectively. The relative grain growth quotient D/D_o for the used starting powder was almost ~1. Further XRD investigations indicated no obvious anatase–rutile transition was found in the prepared nano-crystalline ceramics.

Keywords: A. Grain growth; A. Sintering; B. Grain size; D. TiO_2

1. Introduction

A nano-crystalline ceramic is a dense material with a mean crystallite size below 100 nm. Nano-crystalline ceramics exhibit ductility at low temperature, which is critical for the fabrication of ceramic components. A literature overview on sintering of nano-crystalline TiO_2 reveals that dense rutile, two-phase anatase–rutile or pure anatase nano-ceramics can be obtained via various techniques including classical sintering, hot pressing and sintering forging, among which the typical and prevailing sintering processes are two-step sintering (TSS) and spark plasma sintering (SPS) [1–6]. Several researchers have successfully applied the two-step sintering procedure to synthesize titania nano-ceramics [7,8]. A few others have used spark plasma sintering with the same purpose [9,10]. These studies demonstrate that both of them are successful in densifying TiO_2 ceramics with a reduction in grain size. However, till the present time, almost all the reported TSS experiments are carried out under the conventional sintering conditions. In most cases, the relative grain growth quotient D/D_o for the used starting powder is usually high when TSS was applied. SPS is a process which makes use of microscopic electrical discharge between particles under pressure and so a combination of the hot-press and the plasma generator. This process enables a compact powders to be sintered under uniform heating to high density at relatively low temperature and in a much short sintering periods typically a few minutes. These characteristics make it possible that both high density and refrained grain growth can be achieved at relatively low T_1 if TSS was operated under SPS conditions. However, up to now, no attempts of TSS operation by SPS are found in the opened literatures. So, in the present study, we design a system of significant grain growth suppression based on simultaneous TSS and SPS. Different regimes are envisaged to reveal the role of a combined TSS/SPS procedure on the grain growth and micro-structural evolution of the titania nano-ceramic.

* Corresponding author at: School of Energy, Power and Mechanical Engineering, North China Electric Power University, Beijing 102206, PR China.
E-mail address: libr@ncepu.edu.cn (B.-r. Li).

0272-8842/$36.00
doi:10.1016/j.ceramint.2012.01.011

2. Experimental procedure

In the present study commercial ceramic powders of TiO_2 were used as the raw materials, which were of AR grade (analytical reagent). The TiO_2 powder was spherical and slight agglomerated with an average particle size of 30–40 nm. SEM of TiO_2 nano-powder was given in Fig. 1. The titanium oxides powders were ball-milled with zirconia balls in ethanol for 10 h. After drying, the powders were passed through a 200-mesh sieve. About 2.5–3.0 g of the as-received powders was loaded without any pressure or sintering aids into a graphite die with a diameter of 10 mm and then directly reactive-sintered using an SPS-1050 apparatus (Sumitomo Coal Mining, Japan). A low internal pressure was applied at the beginning of the sintering experiment. During the sintering process the pressure increases to 30 Pa while reaching maximal temperature. The pressure applied at the punch unit reached a maximum of 7–15 MPa.The temperature was measured by means of a pyrometer on the surface of the graphite die cylinder. A temperature gradient between the measured temperature and the sample is expected. The heating rate was at 100 °C/min; the dwelling time was kept from 1 min to 60 min. In order to remove the carbon contamination, the as-prepared pellets were annealed in air at 600 °C for 5 h.

The determination of the density of the compacted samples was performed using Archimedes' principle with ethanol as a liquid medium. The phase characterization of the samples and the subsequent crystallite size determination with X-ray powder diffractometry were performed using an X-ray diffractometer (XRD, *D*/max-RB, Japan) using copper Kα radiation at 40 kV and 40 mA. The micro-structural investigation of the fracture surface of the compacted samples was conducted by using a scanning electron microscopy (SEM 6700 Japan).

3. Results and discussions

Fig. 2 indicates the relative densities and the grain sizes of a normally SPS sample versus the sintering temperatures. The dwelling time is 1 min. It is easily found from Fig. 2 that an explosive grain growth accompanied by densification occurs at the final stage of sintering where density increases from 90% t.d. to 98% t.d. (t.d.: theoretical density). A dense titanium oxides ceramics with the grain size of about 150 nm can be obtained at 950 °C. The relative grain growth quotient D/D_o for the used starting powder is about 4–5 where D_o is the size of the used powders and D is the grain size of the obtained nano-crystalline TiO_2 ceramics. The similar result was also found by P. Angerer and Jun Hong Noh et al. [5,10]. In order to find how effectively the combined TSS–SPS would hinder grain growth, TSS under SPS conditions was explored in our studies. The sintering schedule of TSS procedure is characterized by two regimes wherein the first regime at peak temperature (T_1) dominates densification and complete elimination of residual porosity followed by a second regime at significantly lower temperatures (T_2) effecting controlled grain growth during final stages of sintering. So the efficiency of TSS is mainly dependent on the appropriate choice of T_1 and T_2. The temperature of the first sintering step for TiO_2 is able to be decided on the basis of Fig. 2. According to the reports [7], the density at T_1 should reach a critical value below which no remarkable densification occurring at T_2 is usually possible. It was reported that temperature guaranteeing relative densities between 75% t.d. and 92% t.d. should be chosen for the first sintering step (T_1). According to such a criterion, the corresponding temperature region for T_1 is marked by dashed lines in Fig. 2, in which the grain size is also found to be independent of temperature.

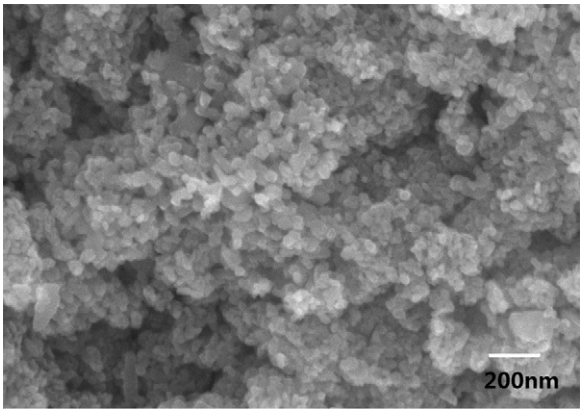

Fig. 1. SEM of the starting TiO_2 powders.

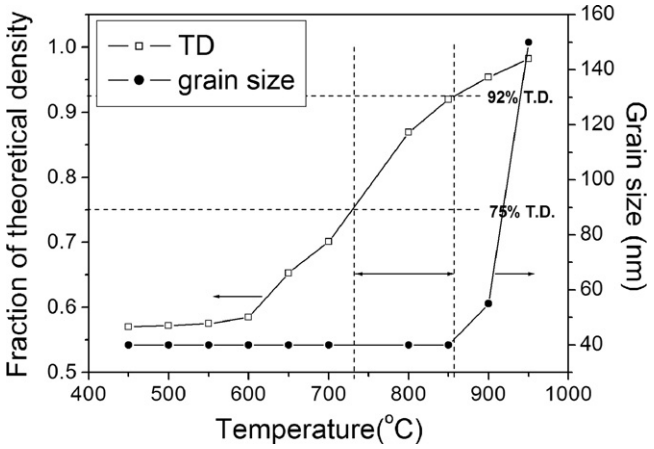

Fig. 2. The dependence of relative densities and grain sizes on the sintered temperatures.

The temperature of the second sintering step is lower than T_1. T_2 can assure the residual subcritical and unstable pores against shrinkage after the first sintering step of TSS is eliminated in the following prolonged sintering. That is to say, in order to obtain a fully dense structure, densification mechanisms of the second sintering step should assure that without applying any pressure, complete densification is able to occur at a lower temperature without any significant grain growth as the holding time is sustained. Various systems have been investigated engaging TSS and the technique was proven successfully for sintering ceramics with controlled grain sizes since it was first reported by Chen and Wang in 2000 [11].

However, some researchers also have found that for some materials such as alumina, would never be densified even after prolonged heat treatment in spite of its starting density of lower than 92% TD [7]. So in order to find appropriate T_2 under SPS conditions, the compact TiO_2 powders were heated at different temperature with a sustained isothermal time. The relative density and the grain size versus the sintering time at various temperatures are displayed in Fig. 3(a). Drawing on the data from the literature, the decrease from T_1 to T_2 was tested in the range of 30–150 °C [11]. So, the temperature in Fig. 3(a) is chosen from 700 to 850 °C. Considering the characterization of SPS instrument, such as fast heating rate, promoted densification rate and short sintering time during SPS process, the holding time at T_2 was designed from 1 min to 60 min. Fig. 3(a) implies the increase of density in the second step of TSS could be achieved when T_2 was higher than 810 °C. Fig. 3(b) is the corresponding dependence of grain size on the calcinations time at different temperatures. Do is the size of the used powders. D is the grain size of nano-crystalline TiO_2 powder compacts sintered at different temperature while the dwelling time is 60 min. Fig. 3(b) indicates the growth of grains is limited if the temperature of the second sintering step is below 840 °C. Based on the above analysis of Fig. 3, it is reasonable to infer that the combination of SPS with TSS can yield a body of identically high density but with a suppressed grain growth. The optimistic T_2 should be in the range from 810 °C to 840 °C.

Fig. 4 shows SEM micrographs of the samples sintered under: (a) SPS at 950 °C, 1 min (b) SPS-assisted TSS condition, T_1 850 °C, T_2 830 °C while the dwelling time is 60 min. High magnification SEM image of the sample is shown in inset of Fig. 4(b). In comparison with sample (a) (95.2% t.d.), higher relative density can be obtained in sample (b) (97.7% t.d.) while no obvious grain growth is found. For further investigations on the efficiency of the combination of TSS with SPS, the other set of TSS experiments under SPS conditions were done by adjusting T_2 to be 810, 820 and 840 °C, respectively, while T_1 is still taken as 850 °C. The obtained SEM micrographs of the samples are shown in Fig. 5. By making comparison with Fig. 4, it can be seen that no obvious changes in both the grain sizes and shape are found in samples sintered at low T_2 temperature (shown as Fig. 5(a) and (b)), but higher T_2 value leads to abnormal grain growth, which is easily observed in Fig. 5(c). The resulting density and grain size for the specimens on different sintering conditions are summarized in Table 1. The results shown in Table 1 indicate that the sample with lower T_2 always present a lower density regardless the holding time in the second step. It is confirmed that setting T_2 at 830 °C is the

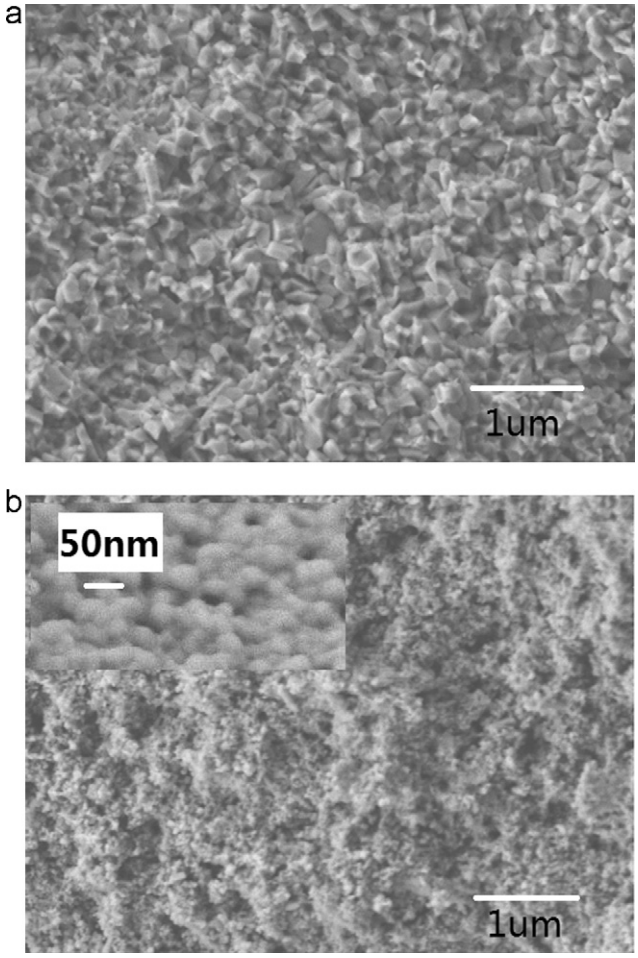

Fig. 4. SEM micrographs of the samples prepared from different sintering patterns (a) SPS at 950 °C, 1 min (b) SPS-assisted TSS condition, T_1 850 °C, T_2 830 °C.

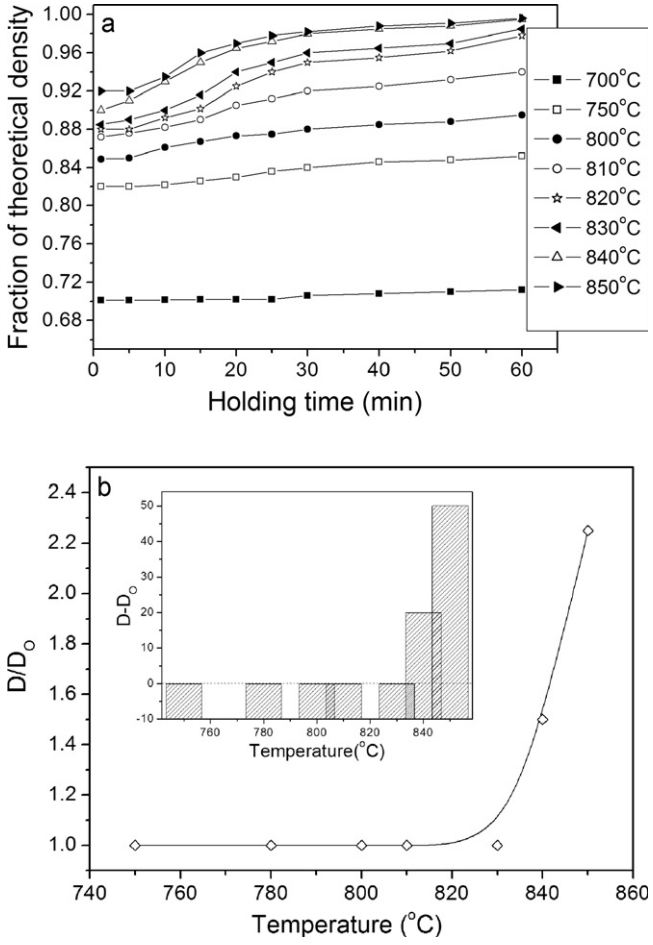

Fig. 3. (a) The relative density of the samples sintered at different temperatures for various holding time and (b) the temperature dependence of D/D_o.

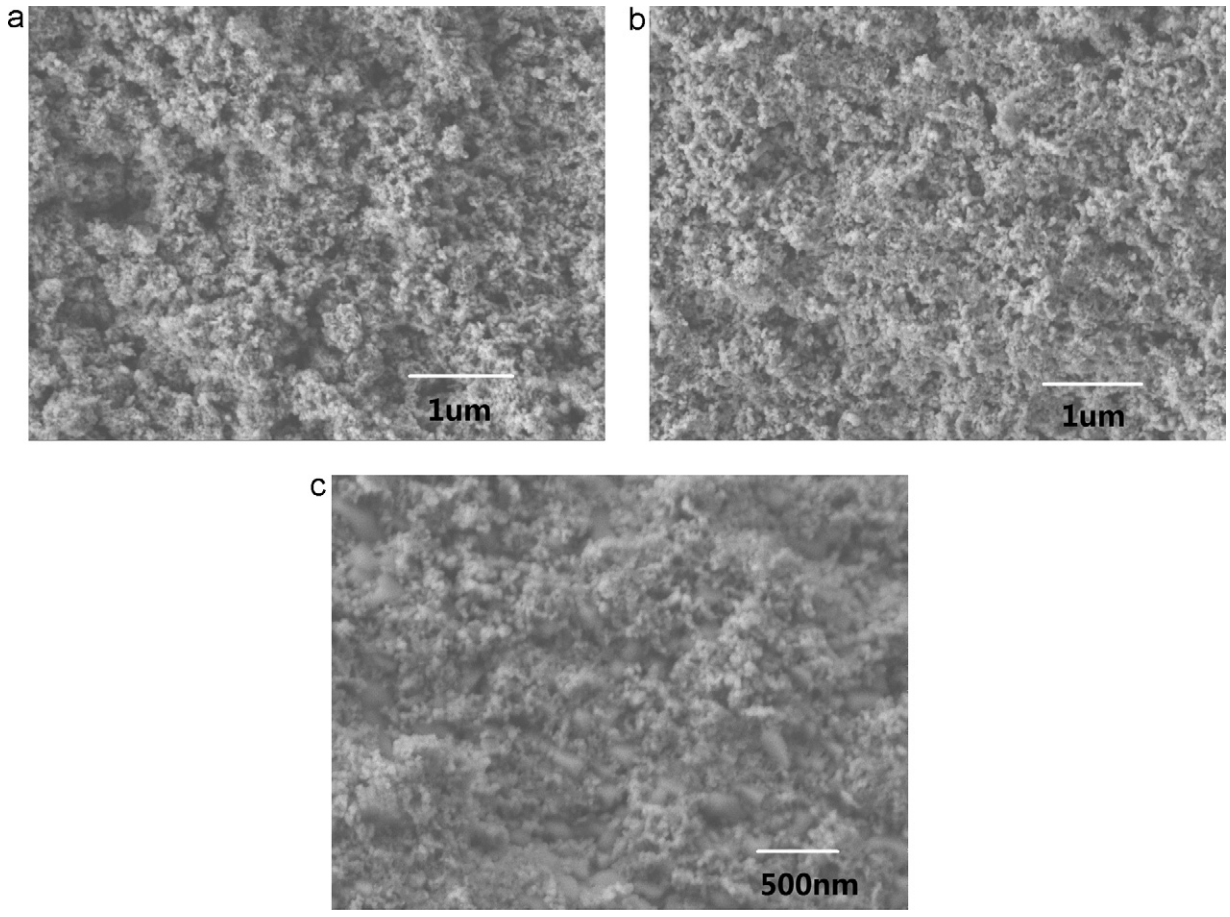

Fig. 5. SEM micrographs of the samples prepared from different sintering patterns (a) SPS-assisted TSS condition, T_1 850 °C, T_2 810 °C while the dwelling time was 60 min. (b) SPS-assisted TSS condition, T_1 850 °C, T_2 820 °C while the dwelling time was 60 min. (c) SPS-assisted TSS condition, T_1 850 °C, T_2 840 °C while the dwelling time was 60 min.

best choice that allows saving the holding time for the second step to achieve the full density. In Fig. 6 the dependence of the grain growth D/D_o as a function of the relative density is shown. For clarity, the selected part between the dashed lines 1 and 2 is enlarged in the set of Fig. 6. The grain growth in TSS–SPS experiments is shown to be significantly lower in comparison to the other samples with an equivalent degree of densification. Fig. 7 summarizes the reported processing methods (the separated TSS or SPS operation shown in Refs. [2,5,12–15,10,16–21]) and their influence on the relative densities and grain growth quotient D/D_o. A magnified view of a selected part between lines 1 and 2 is shown in the set of Fig. 7, in which the dashed line represents D equal to D_o. Fig. 7 suggests that the relative grain growth quotient D/D_o for the used starting powder is higher than 1 in most cases in spite of varieties of the materials. It was reported that the relative grain growth quotient D/D_o was approach to ~10 when TSS was applied to the sintering of titania nano-ceramic while that of SPS was in the range of 3–6 [5,6,8,10]. However, the relative grain growth

Table 1
Sintered densities and grain size of specimens under various heating parameters of TSS assisted by SPS.

T_1 (°C)	T_2 (°C)	Holding time (min)	Relative density (%)	Grain size (nm)
850	810	60	94.5	40
850	820	60	95.2	40
850	830	60	97.7	40
850	840	60	99.1	–

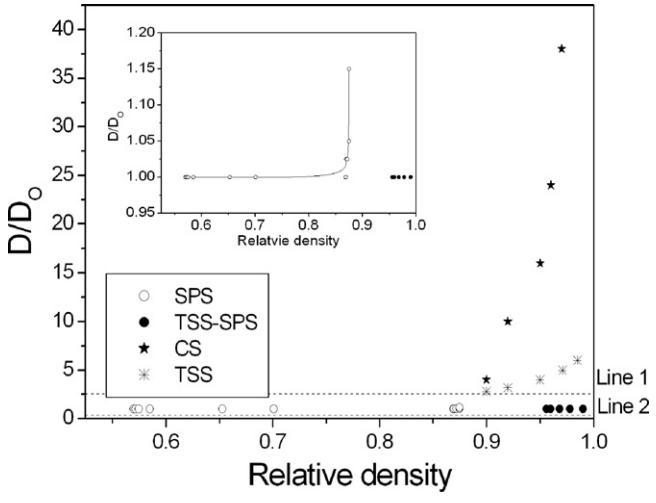

Fig. 6. The dependence of the grain growth D/D_o on the relative density.

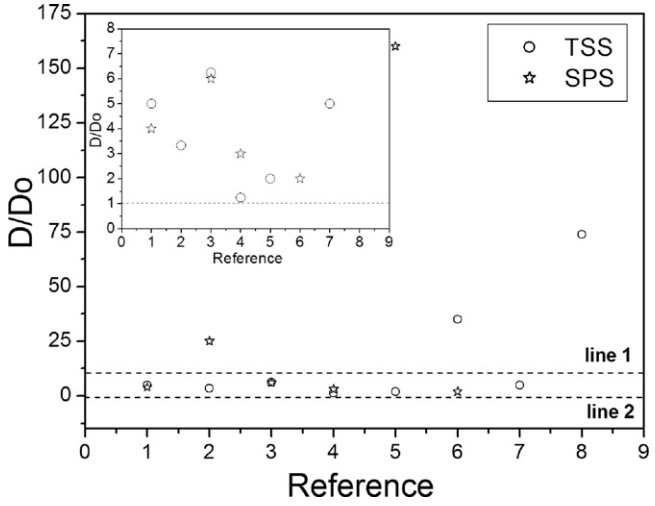

Fig. 7. The influences of the processing methods on grain growth quotient D/D_o. The relative densities of all the presented samples are higher than 95% t.d.

quotient D/D_o for the used starting powder is only ~1 under SPS assisted by TSS. These facts suggested SPS modified by TSS was more efficiency than the separated TSS or SPS operation.

According to the solid state sintering mechanism, dispersed open pores could pin grain boundaries and hider grain boundary migration, for which the grain growth was suppressed when the relative density is between 65 and 90% t.d. However, a considerable grain growth could take place in the final stage of sintering while at the same time no remarkable increase in density was produced. This is because the collapsed open pores in the final stage of sintering could weaken the pore pinning, further resulting in the accelerated grain growth [22]. TSS employing longer heat treatment, while reducing the firing temperature, was reported to be able to suppress the grain growth happened in the final stage of sintering effectively [11]. But there is a critical temperature for the second step as well as for the first one in two-step sintering tests. Moreover, the relative density of the sample obtained by isothermal dwelling at T_2 strongly depends on the peak temperature T_1. Low temperatures (T_1 or T_2) fail to eliminate the residual porosity of samples while high temperatures (T_1 or T_2) easily lead to an accelerated grain growth. In order to make an enhancement in density without significant grain growth having to occur, both T_1 and T_2 should be kept as low as possible if the critical value obtained at T_1 could be satisfied and further densification process at T_2 is not interrupted. This usually makes the right choice of T_1 very difficult under the conventional sintering conditions. Another shortcoming of TSS is the prolonged annealing time in the second step temperature, which has seriously questioned the application of this method on some special occasions although TSS is reputed as a successful approach to avoid the accelerated grain growth. All these questions are expected to be solved by the combination of TSS with SPS. The most important feature of SPS is the efficiency of heat-treatment. The graphite die heated directly by an electric current results in rapid heating and cooling. Fast firing postpones reaching the activation energy required for the grain boundary mobility as the major cause of grain growth to the higher temperatures. So, it can suppress the grain coarsening effectively and further result in high density because the increase of densification rate can take place either by the increase of $\delta_b D_b$ or the decrease of G according to the following equation, in which the influence of sintering heating rate on the micro-structural evolution of the sintered specimens can be described:

$$\frac{d\rho}{dt} = \frac{C\gamma_s D N_g}{G^n} \quad (1)$$

where ρ is density, C is a constant, and γ_s is the solid/gas surface energy; D represents either the lattice diffusion coefficient (DL) or the grain boundary diffusivity $(\delta_b D_b)$, where δ_b is the grain boundary width and D_b is the grain boundary diffusion coefficient, N_g is the number of boundary pores per grain, and G is the grain size.

Another expected merit of SPS is generation of spark plasma created by a pulse direct current during heat treatment of powders in a graphite die. The pressed powders are heated by the spark discharge between the particles. A volumetric heating is produced in the whole bulk of the material. This is different from the heating style in the conventional sintering, in which the surface of the material is heated sooner than the core [23]. So compared with the conventional sintering method, the SPS process enables a compact powders to be sintered under uniform heating to high density at relatively low temperatures and in a much shorter sintering periods. When TSS is combined with SPS, the fast heating and cooling rate of SPS can lower T_1 and T_2 of TSS significantly and lowered sintering temperature carried out in the SPS process are advantageous in suppressing exaggerated grain growth and further improve the efficiency of TSS.

A phase transition of anatase into rutile is detected by XRD for the powders sample densified at the temperatures from 800 to 850 °C with the dwelling time of 1 and 60 min. The results are shown in Fig. 8. The dashed lines represent the most intense diffraction lines of the rutile phase. Using the relative intensities of the most intense (1 0 1) peak of anatase and (1 1 0) peak of rutile, the composition of rutile phase content with synthesis temperature is described in Fig. 8(b). It is easily found that the onset of the anatase to rutile transformation by SPS is at temperature higher than 850. Also the transformation of nano-crystalline anatase to rutile at constant temperature is affected greatly by the dwelling time, as shown in samples (d) and (e) in Fig. 8(a). At 850 °C, the amount of rutile increase from 1.5% to 17.8% when the dwelling time changes from 1 min to 60 min. However, the transition becomes extremely sluggish at temperatures lower than 850 °C even if the holding time is increased to 60 min. The above results suggest bulk titania nano-ceramics with pure anatase or anatase accompanied with minimal amount of rutile can be obtained by the combination of TSS with SPS because the first sintering step (T_1) in our studies is as low as 850 °C and the corresponding holding time is only 1 min. This assumption is further

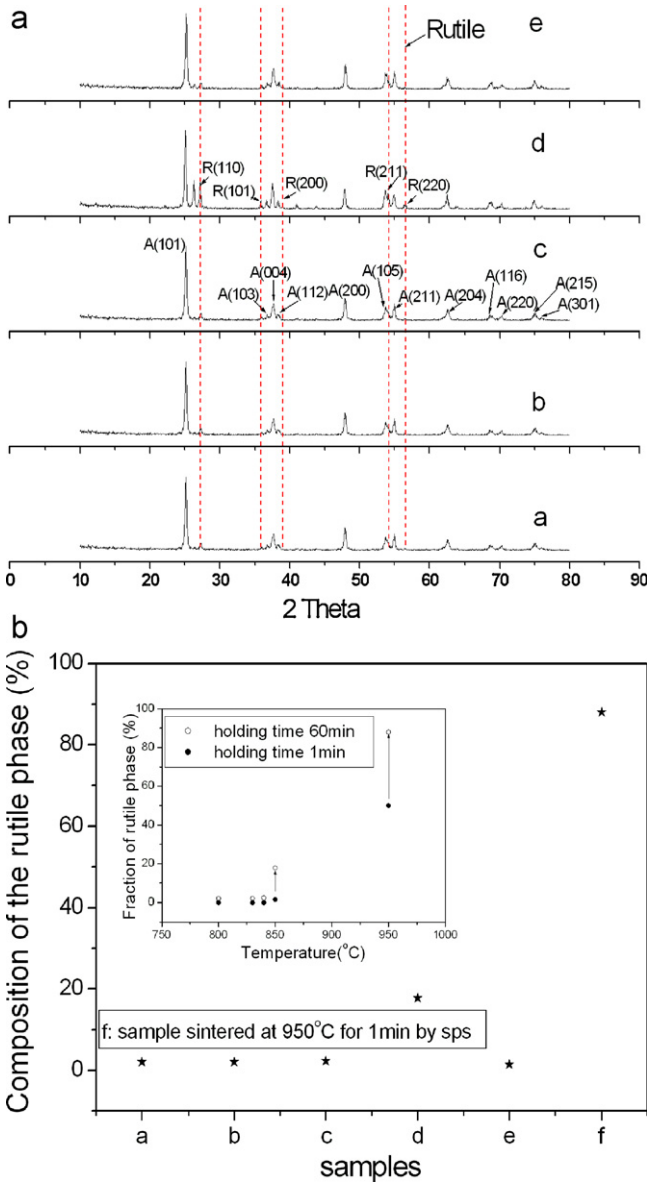

Fig. 8. (a) X-ray diffraction patterns for samples sintered at different temperatures. A denotes anatase phase, R denotes rutile phase: (a) 800 °C/60 min; (b) T_1 = 850, T_2 = 830 °C, holding time is 60 min; (c) 840 °C/60 min; (d) 850 °C/60 min; (e) 850 °C/1 min; (b) variations of the rutile phase as a function of calcinations temperature.

confirmed by the actual XRD analysis on the sample (b) in Fig. 8.

The anatase to rutile transition has been studies extensively and it is generally accepted that the transformation takes place in the temperature range from 400 to 1000 °C depending upon a variety of factors including crystalline size, size distribution, contact area of crystallites in the powder, impurity type and concentration, and atmosphere [24]. Moreover, it was also reported that anatase was stable at small grain size and the critical size values, corresponding to the beginning of phase transition into rutile, varied between 10 and 50 nm [4]. These suggest the stabilization of anatase at temperatures lower than 850 °C in our studies might have close relations to the small grain size resulting from suppressed grain growth. So the similar compositions in samples a, b, c and e, mainly composed of anatase phase, could be found. In comparison with samples a, b, c and e, the increased amounts of rutile in samples d and f can be attributed to relative longer annealing time and higher calcinations temperature because the long calcinations time and high temperature can effectively control the rutile phase of TiO_2 [25].

4. Conclusions

In summary, the present study shows the formation of nano-grains during two-step sintering of titania nano-ceramics assisted by the well-known SPS. The grain sizes of the normally SPS samples were 200 nm or so. By taking the benefits of combined SPS–TSS effects, a structure with finer grain sizes of around 40 nm was obtainable. Moreover, further analysis of XRD suggested the anatase phase was able to stabilize in the sample because of the relative lower sintering temperatures in comparison with SPS. These results confirmed SPS assisted by TSS could suppress the grain growth more effectively than the separated TSS or SPS operation.

References

[1] H.G. Kim, K.T. Kim, Densification behavior of nano-crystalline titania powder compact under high temperature, Acta Mater. 47 (1999) 3561–3570.
[2] K. Maca, V. Pouchly, P. Zalud, Two-step sintering of oxide ceramics with various crystal structures, J. Eur. Ceram. Soc. 30 (2010) 583–589.
[3] S.C. Liao, Y.J. Chen, W.E. Mayo, High pressure/low temperature sintering of nanocrystalline alumina, Nanostruct. Mater. 11 (1999) 553–557.
[4] A. Weibel, R. Bouchet, R. Denoyel, P. Knauth, Electrical properties and defect chemistry of anatase (TiO_2), J. Eur. Ceram. Soc. 27 (2007) 2641–2646.
[5] J.H. Noh, H.S. Jung, J.-K. Lee, J.-R. Kim, Microwave dielectric properties of nanocrystalline TiO_2 prepared using spark plasma sintering, J. Eur. Ceram. Soc. 27 (2007) 2937–2940.
[6] N. Masahashi, Fabrication of bulk anatase TiO_2 by the spark plasma sintering method, Mater. Sci. Eng. A 452–453 (2007) 721–726.
[7] M. Mazaheri, Z. Razavi Hesabi, S.K. Sadrnezhaad, Two-step sintering of titania nanoceramics assisted by anatase-to-rutile phase transformation, Scripta Mater. 59 (2008) 139–142.
[8] M. Mazaheri, A.M. Zahedi, M. Haghighatzadeh, S.K. Sadrnezhaad, Sintering of titania nanoceramic: densification and grain growth, Ceram. Int. 35 (2009) 685–691.
[9] Y.I. Lee, J.-H. Lee, S.-H. Hong, Preparation of nanostructured TiO_2 ceramics by spark plasma sintering, Mater. Res. Bull. 38 (2003) 925–930.
[10] P. Angerer, L.G. Yu, K.A. Khor, G. Krumpel, Spark-plasma-sintering (SPS) of nano-structured and submicron titanium oxide powders, Mater. Sci. Eng. A 381 (2004) 16–19.
[11] W. Chen, X.H. Wang, Sintering dense nanocrystalline ceramics without final-stage grain growth, Nature 404 (2000) 168–171.
[12] Y. Zheng, S.X. Wang, Y.L. Yan, N.W. Zhao, X. Chen, Microstructure evolution and phase transformation during spark plasma sintering of Ti(C N)-based cermets, Int. J. Refract. Met. Hard Mater. 26 (2008) 306–311.
[13] L. Gao, J.S. Hong, H. Miyamoto, S.D.D.L. Torre, Bending strength and microstructure of Al_2O_3 ceramics densified by spark plasma sintering, J. Eur. Ceram. Soc. 20 (2000) 2149–2152.
[14] L. Bao, J. Zhang, S. Zhou, Effect of particle size on the polycrystalline CeB_6 cathode prepared by spark plasma sintering, J. Rare Earth 29 (2011) 580–583.

[15] I. Akin, M. Hotta, F.C. Sahin, O. Yucel, G. Goller, T. Goto, Microstructure and densification of ZrB_2–SiC composites prepared by spark plasma sintering, J. Eur. Ceram. Soc. 29 (2009) 2379–2385.
[16] J. Ma, S. Zhu, C. Ouyang, Two-step hot-pressing sintering of nano-composite WC–MgO compacts, J. Eur. Ceram. Soc. 31 (2011) 1927–1935.
[17] M.M. Shahraki, S.A. Shojaee, M.A.F. Sani, A. Nemati, I. Safaee, Two-step sintering of ZnO varistors, Solid State Ionics 190 (2011) 99–105.
[18] M.H. Fathi, M. Kharaziha, Two-step sintering of dense nanostructural forsterite, Mater. Lett. 63 (2009) 1455–1458.
[19] Z. Razavi Hesabi, M. Haghighatzadeh, M. Mazaheri, D. Galusek, S.K. Sadrnezhaad, Suppression of grain growth in sub-micrometer alumina via two-step sintering method, J. Eur. Ceram. Soc. 29 (2009) 1371–1377.
[20] S.H. Kim, J.W. Kim, T.S. Jo, Y.D. Kim, High coercive Nd–Fe–B magnets fabricated via two-step sintering, J. Magn. Mater. 323 (2011) 2851–2854.
[21] M. Lukić, Z. Stojanović, S.D. Škapin, M. Maček-Kržmanc, M. Mitrić, S. Marković, D. Uskoković, Dense fine-grained biphasic calcium phosphate (BCP) bioceramics designed by two-step sintering, J. Eur. Ceram. Soc. 31 (2011) 19–27.
[22] X.H. Wang, P.L. Chen, I. Chen, Two-step sintering of ceramics with constant grain-size. I. Y_2O_3, J. Am. Ceram. Soc. 89 (2006) 431–437.
[23] M. Mazaheri, A.M. Zahedi, M.M. Hejazi, Processing of nano-crystalline 8 mol% yttria-stabilized zirconia by conventional microwave-assisted and two-step sintering, Mater. Sci. Eng. A 492 (2008) 261–267.
[24] J.-G. Li, T. Ishigaki, Brookite → rutile phase transformation of TiO_2 studied with monodispersed particles, Acta Mater. 52 (2004) 5143–5150.
[25] M.S. Nahar, J. Zhang, K. Hasegawa, S. Kagaya, S. Kuroda, Phase transformation of anatase–rutile crystals in doped and undoped TiO_2 particles obtained by the oxidation of polycrystalline sulfide, Mater. Sci. Semiconduct. Process. 12 (2009) 168–174.